EPR and NMR spectroscopy of spin-labeled proteins

Finiguerra, M.G.

Chapter II

High-field (275 GHz) spin-label EPR for high-resolution polarity determination in proteins

Abstract

The polarity of protein surfaces is one of the factors driving protein-protein interactions. High-field, spin-label EPR at 95 GHz, i.e., a frequency 10 times higher than for conventional EPR, is an upcoming technique to determine polarity parameters of the inside of proteins. Here we show that by 275 GHz EPR even the small polarity differences of sites at the protein surface can be discriminated. To do so, four single cysteine mutations were introduced at surface sites (positions 12, 27, 42 and 118) of azurin and spin labeled. By 275 GHz EPR in frozen solution, polarity/proticity differences between all four sites have been resolved, which is impossible by 95 GHz EPR. In addition, by 275 GHz EPR, two spectral components are observed for all mutants. The difference between them corresponds to one additional hydrogen bond.

The results in this chapter have been published in:

Finiguerra M. G. , Blok H., Ubbink M., Huber M. High-field (275 GHz) spin-label EPR for high-resolution polarity determination in proteins. *Journal of Magnetic Resonance* **180**, 187-202 (2006)

Introduction

Protein-protein interactions are driven by the properties of the respective protein surfaces, for example, the polarity of the surface. Therefore, methods to determine the polarity of protein surfaces experimentally are sought. Spin-label, high-field EPR has proven useful to determine polarity parameters of the interior of proteins. To do so, a spin label is placed at the position of interest in the protein. The EPR parameters of the spin label reflect the polarity and proticity of the environment of the spin label, where proticity refers to the propensity of the protein environment to donate hydrogen bonds. Placing the spin label at different positions in the protein enables determination of the protein polarity locally. To obtain sufficient spectral resolution, EPR spectroscopy performed at high magnetic fields and microwave frequencies is advantageous. As an example, by EPR performed at 3 T and 95 GHz (W-band), i.e., at 10 times higher fields and frequencies than conventional 9 GHz (X-band) EPR, polarity profiles of membrane proteins have been determined[1]. In order to discriminate between positions of similar polarity, such as expected for positions at the surface of the protein, it is important to be able to perform EPR at even higher magnetic fields and frequencies. Several 250 GHz EPR studies have been reported for model systems of biological membranes using spin-labeled lipids with the focus on dynamics rather than polarity[2]. Experiments to determine polarity by EPR at fields higher than 95 GHz on spin-labeled proteins have only recently been performed, namely by EPR at 360 GHz (K. Möbius *et al.*, private communication).

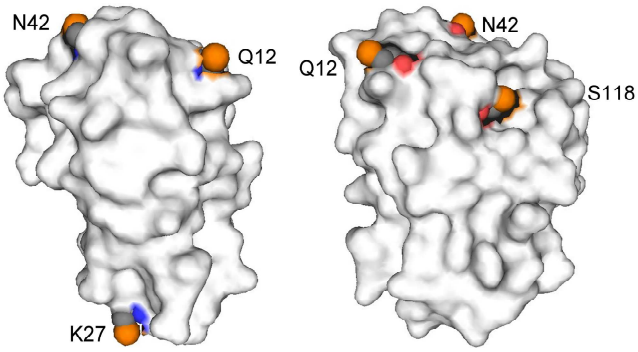

Figure 2.1 Location of the mutated residues. Azurin is depicted in surface representation (grey). The residues mutated in this study are shown as Cys residues, with the sulfur in orange. The right view is rotated by 90° around the vertical axis relative to the left one.

In the present study, spin labels were introduced at positions close to the surface of the protein by spin label mutagenesis[3]. Four single mutants of a protein of known structure, azurin (Figure 2.1), were prepared. To avoid interference from the paramagnetic Cu(II) of azurin, the metal ion was replaced by Zn(II), Zn-azurin. To obtain sufficient resolution for the small differences in polarity and proticity expected, we employed an EPR spectrometer operating at 9 T and 275 GHz (J-band)[4] which is designed to provide the high sensitivity needed for the study of biological samples. The data were compared with those obtained using a commercial W-band EPR spectrometer.

The EPR experiments reveal that even the small differences in polarity of these mutants become detectable at 275 GHz. The most striking result is that in the spectra of all mutants two spectral components are observed that can not be resolved by W-band EPR.

Materials and methods

Four mutants of Zn-azurin (azurin with Cu(II) replaced by Zn(II)) containing a surface exposed cysteine residue have been prepared. The N42C mutant[5] and the K27C and S118C mutants were prepared as described in ref. 9, the preparation of the Q12C mutant will be described elsewhere (S. Alagaratnam, unpublished results). The procedure for spin labeling these mutants is also described in ref. 9.

Sample preparation and measurements

The concentration of the samples used was between 0.8 and 1.2 mM. The volume used for W-band EPR measurement was about 0.8 μl including 30% glycerol, and the sample was introduced into a Wilmad suprasil quartz tube with an inner diameter (i.d.) of 0.60 mm and an outer diameter (o.d.) of 0.84 mm, from Wilmad-Labglass (Buena, NJ, USA) sealed at one end. The W-band measurements were performed at 40 K and the sample was frozen directly by introduction into the cryostat.

The volume used for J-band EPR measurement was about 17 nl including 50% glycerol. The sample was measured in a locally made quartz capillary with i.d. of 0.15 mm and o.d. of 0.3 mm. Measurements were performed at 100 K. The modulation frequencies were 100 kHz (W-band) and 2 kHz (J-band); modulation amplitude: 0.5 mT (W-band) and 1 mT (J-band); microwave (mw) power: 8 nW (W-band) and 10 μW (J-band); total measurement time: 20 min (W-band) and 9 min (K27 and Q12), respectively, 17 min (S118 and N42) (J-band).

Instrumentation

For W-band EPR experiments a Bruker Elexsys 680 (Bruker Biospin GmbH Rheinstetten, Germany) spectrometer and for J-band EPR experiments a laboratory-designed spectrometer[4] was used.

Spectral simulations

The program used for simulations was SimFonia (Bruker-Biospin, Rheinstetten). Errors of parameters have been determined by changing each parameter by the smallest possible amount that produced a visible deterioration of the quality of the simulation with respect to the spectrum. For

the unresolved hyperfine couplings A_{xx} and A_{yy}, in the simulation of the W- and J-band EPR spectra the following values were used. The A_{xx} values were: Q12C 0.50 mT, K27C 0.50 mT, N42C 0.48 mT and S118 0.43 mT. The A_{yy} values were: Q12C 0.50 mT, K27C and N42C 0.48 mT, and S118 0.45 mT. The error in A_{xx} and A_{yy} is ±0.03 mT, except for A_{xx} of Q12C in J-band EPR, where it is ±0.05 mT. The simulation parameters A_{xx} and A_{yy} depend on the component linewidth used in the simulation, which was fixed at 0.82 mT for W-band simulations and at 1.6 mT for J-band simulations.

The EPR parameters obtained from the J-band and the W-band EPR spectra should be identical. Nevertheless, the A_{zz} values obtained from J-band EPR were systematically lower (by 0.05 to 0.08 mT) than those from W-band EPR. With a Mn(II) standard sample we observed a deviation in the same direction, suggesting that the calibration of the slope of the field sweep (dB/dI, with B the static magnetic field, and I, the magnet current) of the J-band EPR magnet differs from that of the W-band magnet. The difference in the slope calibration observed on the standard sample corresponds to a correction of +0.024 mT for the A_{zz} values from J-band EPR. The same re-calibration applied to the field separation between the g_{zz} and the g_{xx} (and the g_{yy}) component results in a correction by $+4 \times 10^{-5}$ for g_{xx} and by $+3 \times 10^{-5}$ for g_{yy} for the values from J-band EPR. The parameters from J-band EPR in Table 2.1 are corrected accordingly. Remaining differences in the W-band and the J-band EPR parameters can be attributed to the differences in temperature, which was 100 K in the J-band EPR and 40 K in the W-band EPR experiments, and in glycerol content, i.e., 50% in J-band EPR and 30% in W-band EPR experiments. We measured for two of the mutants (K27C and S118C), that A_{zz} at 100 K is smaller by ca. 0.03 mT than at 40 K. At 50% glycerol content, A_{zz} is larger by ca. 0.06 mT than at 30%. Combining both effect, for the measurement conditions in the J-band EPR experiments, a differences of +0.03 mT is expected for A_{zz} compared to A_{zz} from W-band EPR. The differences in temperature also seems to affect the g_{xx} values, since, at 100 K, the Q12C sample (50% glycerol content, measured by J-band EPR) had a g_{xx} (av) value that was larger by 3×10^{-5} than g_{xx} (av) at 40 K.

Results

Mutants of azurin with spin labels at positions 12, 27, 42, and 118 (Q12C, K27C, N42C, and S118C) have been investigated. The EPR measurements were performed on frozen solutions of the spin-labeled mutants using W-band and J-band EPR.

In Figure 2.2, the EPR spectra at J-band of the spin label in all four mutants of the Zn-azurin are shown. The resonance field positions for B_0 along the nitroxide *x*-, *y*- and *z*-axes of the g tensor are indicated. The W-band EPR spectra of frozen solutions of all mutants were measured, and in Figure 2.2 one of these, the spectrum of S118C is shown. Compared with the W-band spectra, the J-band spectra have a higher resolution. This can be seen by the larger separation of the group of three lines that are centered at g_{zz} and separated by A_{zz}, and the peak at g_{yy}. The overlap of the lower field A_{zz} line with the g_{yy} feature in the W-band spectra causes an additional peak at the high field side of the g_{yy} band (see S118 W-band EPR spectrum, Figure 2.2). That feature is difficult to simulate as it depends on a combination of simulation parameters. Moreover, in the J-band spectra, a splitting of the EPR signal at g_{xx} into two components, g_{xx} (I) (the larger g_{xx}-value that appears at lower field) and g_{xx} (II) (the smaller g_{xx}-value that appears at higher field), becomes visible. This splitting is most clearly seen in the spectrum of the S118C mutant, Figure 2.2.

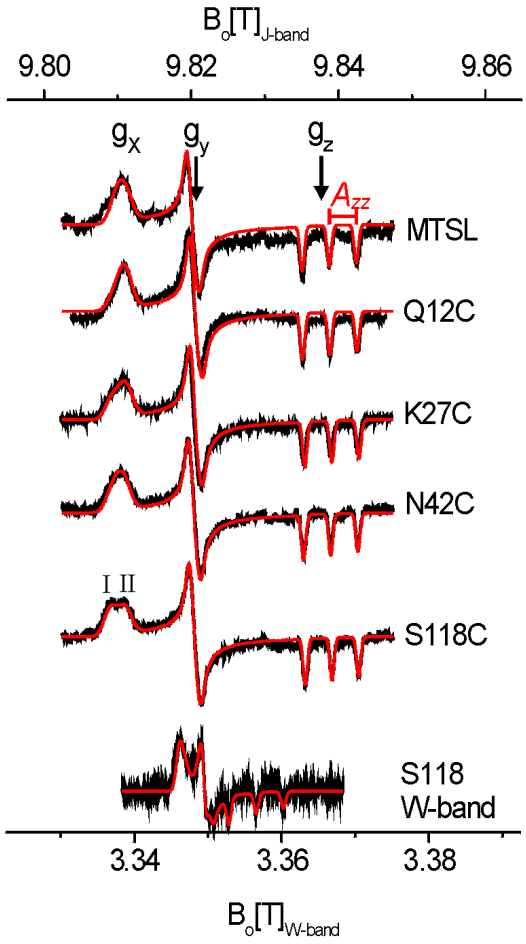

Figure 2.2 J-band EPR spectra of azurin mutants and W-band spectra of S118 mutant at 40K (W-band) and 100K (J-band). Arrows at g_{xx}, g_{yy} and g_{zz} : resonance for magnetic field along the g-tensor x-, y-, and z-axes. A_{zz}: nitrogen hyperfine coupling along z-direction. Simulation for all spectra are shown (dotted lines).

To analyze this spitting, the J-band EPR spectra were simulated with two spectral components, which differ only with respect to the g_{xx} values and the relative contribution of the components to the total spectra. The respective components are given as g_{xx} (I) and g_{xx} (II) in the Table 2.1. To make sure that this splitting is not an artifact, simulations of the W-band spectra were performed using the two components obtained from J-band EPR.

These simulations agreed with the experimental spectra, confirming that the difference between the g_{xx} (I) and g_{xx} (II) values is too small to be resolved by W-band EPR.

Due to the higher resolution of J-band EPR, the errors in the simulation parameters at J-band are overall smaller than those at W-band. Partly, this is due to the larger separation of the individual components of the spectra. Furthermore, a frequent problem in the W-band EPR spectra of protein samples are signals of Mn(II) impurities. The signal of these impurities overlaps the lines of the spin-label spectra in W-band EPR, thus increasing the experimental errors in determining the position of these lines. This was the case for the W-band EPR spectra of the K27C mutant. In the J-band EPR spectra, the signal of the Mn(II) impurity does not overlap with the spectrum of the spin label, resulting in smaller errors.

Table 2.1 g and hyperfine tensor parameters of azurin mutants from W-band (95 GHz) and J-band (275 GHz) EPR

Mutant	band	g_{xx} (I) [a]	g_{xx}(II) [a]	g_{xx} resp. g_{xx}(av) [b]	g_{yy} [c]	g_{zz}	A_{zz} [d] mT
Q12C	W	n.a.[e]	n.a.	2.00775	2.00574	2.00198	3.77
	J	2.00795(20%)	2.00765	2.00771	2.00567		3.75
K27C	W	n.a.	n.a.	2.00788	2.00583		3.73
	J	2.00806(30%)	2.00769	2.00780	2.00573		3.73
N42C	W	n.a.	n.a.	2.00783	2.00579		3.77
	J	2.00803(35%)	2.00773	2.00783	2.00574		3.75
S118C	W	n.a.	n.a.	2.00794	2.00585		3.70
	J	2.00811(55%)	2.00771	2.00793	2.00576		3.67

For comparison, all g-values are adjusted to g_{zz} = 2.00198. No calibration of absolute g values was performed. Errors of g values are given with respect to the relative magnitude of g_{xx} and g_{yy} vs. g_{zz}:
Error: $\pm 1 \cdot 10^{-5}$. In bracket: percentage of contribution of species.
g_{xx}(av): weighted average of g values g_{xx}(I) and g_{xx}(II) from J-band; errors: $\pm 2 \cdot 10^{-5}$. For Q12, error: $\pm 4 \cdot 10^{-5}$.
g_{xx}: principal value of g-tensor from W-band: only one component used in the simulations; error: $\pm 2 \cdot 10^{-5}$. For K27C, error: $\pm 6 \cdot 10^{-5}$ due to the presence of Mn(II) impurity in the sample.
Error: W-band $\pm 6 \cdot 10^{-5}$; J-band $\pm 3 \cdot 10^{-5}$
Error: ± 0.025 mT for W and J-band spectra except for J-band: K27: ± 0.03 mT. J-band values: 0.045 mT added to account for different magnet field sweep calibrations (see text)
n.a.: not applicable

From J-band EPR, the order of the g_{xx} values, i.e. the weighted average g_{xx} (av) of g_{xx} (I) and g_{xx} (II) of the four mutants is S118C > K27C ≈ N42C > Q12C. The error of the determination of g_{xx} from the W-band spectra was too large to determine that order. The A_{zz} parameters of the four mutants are very similar. The largest A_{zz} values are found for Q12C and N42C. They are significantly larger than the value for S118C. The A_{zz} value of K27C agrees within experimental error with those of the three other mutants, not allowing to place the A_{zz} value of this mutant relative to the other mutants.

A plot of A_{zz} vs. g_{xx} illustrates the polarity/proticity properties (Figure 2.3), where proticity refers to the propensity of the protein environment to donate hydrogen bonds. The squares are values of the spin label MTSL in different solvents from Owenius *et al.*[6]. The dots are the J-band EPR data obtained on the Zn-azurin mutants.

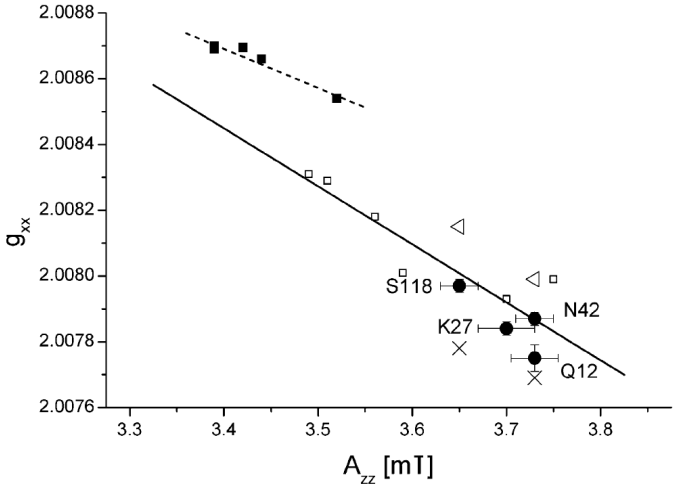

Figure 2.3 Plot of g_{xx} vs. A_{zz} of spin labels in Zn-azurin. Dots: g_{xx}(av) from J-band EPR, triangles: g_{xx}(I), crosses: g_{xx}(II) of S118C and Q12C. For reference the values of MTSL in different solvents are shown (filled squares, aprotic; open square, protic solvents). Dotted line: Linear correlation of g_{xx} vs. A_{zz} for non-hydrogen bonding solvents; solid line, linear correlation for hydrogen bonding solvents [5]. Figure modified from ref [7].

Shown are the values of g_{xx} (av) for all mutants, and for S118C and Q12C also the values of g_{xx} (I) and g_{xx} (II). The mutants are located in a region of the plot where the more protic, polar solvents are found (see Discussion).

Discussion

Spin labels at four surface sites in Zn-azurin are investigated. The higher resolution of J-band EPR reveals the presence of two spectral components, not previously resolved in W-band EPR spectra of spin-labeled proteins. The signal-to-noise ratio of the J-band EPR spectra shows that the sensitivity of this new EPR spectrometer is sufficient to measure biological samples with realistic concentrations, i.e. around 0.5 mM. Remarkable is the very modest volume required for the sample (see Materials and methods), resulting in a total amount of protein needed of only 17 pmol.

The EPR signals can be simulated with regular powder line shapes, revealing the absence of spectral distortions due to dispersion admixture, which is a frequent problem in high-field EPR. Thus, reliable g- and hyperfine tensor parameters were obtained. The EPR results from W-band and J-band EPR are overall consistent (see Table 2.1). The remaining differences between the EPR parameters of the individual mutants derived from W-band and J-band EPR are attributed to the differences in measurement temperature and glycerol content in the two experiments (see Materials and methods). The J-band EPR spectra were simulated with a larger component linewidth, 1.6 mT, compared to 0.82 mT for the W-band EPR spectra, indicating that in addition to unresolved hyperfine couplings, which do not depend on field, g-strain and other inhomogeneities start to play a role at J-band.

The absence of spectral overlap in the J-band EPR spectra permits determination of the g-values with higher precision, enabling us to establish the order of the mutants with respect to g_{xx}, which is impossible by W-band EPR.

Two components of the spin-label spectra that differ with respect to their g_{xx} values can be resolved by J-band EPR. They are separated by $\Delta g_{xx} = 4 \times 10^{-4}$ (g_{xx}(I) - g_{xx}(II)), corresponding to 1.7 mT at that field. In W-band EPR, the same Δg_{xx} amounts to a splitting of ≈0.6 mT. As shown by the simulation of the W-band EPR spectra with two components (see Results) this separation is not large enough to resolve the two components. Previously, separations as small as 2×10^{-4} were resolved by W-band EPR, albeit in systems where spectra with significantly better signal-to-noise ratio could be obtained. One example was the investigation of MTSL in different solvents[6]. At small values of Δg_{xx} in W-band EPR, the second component appears as a shoulder at the low field edge of the spectrum, which cannot be distinguished in spectra of lower signal-to-noise ratio, such as the typical spin-labeled protein.

For the interpretation of the differences in the EPR parameters obtained for the different mutants, a plot of g_{xx} vs. A_{zz} is shown in Figure 2.3. Such plots serve to illustrate polarity/proticity profiles, as g_{xx} is most sensitive to differences in proticity, and A_{zz} to differences in polarity. In Figure 2.3 the data points obtained for the four mutants are compared with the parameters of MTSL in a series of solvents[6]. Unpolar/aprotic solvents are characterized by high g_{xx}/low A_{zz} values, polar/protic solvents by low g_{xx}/high A_{zz} values. Linear correlations of A_{zz} vs. g_{xx} for the data obtained in different solvents are shown. The dotted line corresponds to aprotic, the solid line to protic solvents. In this plot, the spin labels of Zn-azurin are located in a region close to the polar and hydrogen-bond-forming solvents. This agrees with the location of the spin labels close to the surface of the protein. According to the differences in polarity/proticity observed, the spin label in the S118C mutant is in the most apolar/aprotic environment, i.e. S118 is the most buried residue, whereas Q12 and N42 are the most solvent exposed residues. The X-ray structure of azurin[8], reveals that all residues are close to the surface. The difficulty to dimerize S118C-azurin has been interpreted as evidence for a low solvent accessibility of S118[9]. Also, mobility studies performed by W-band EPR reveal a significantly reduced mobility for S118C[10], suggesting that S118 is more buried than the other residues. Interestingly, the mobility of the spin label attached to Q12C is lower than that attached to K27C[10], whereas the present study reveals a more apolar/aprotic, i.e. more buried environment for K27C. This could suggest that the spin label attached to K27C is in a protein pocket that is shielded from outside water, but large enough to allow motion of the spin label. That proposition could be tested by molecular dynamics simulations, for example, but in the absence of those, any structural model has to remain speculation.

The higher resolving power of J-band compared to W-band EPR enables the differentiation of even more subtle differences in proticity. It reveals that each spin-label position in Zn-azurin results in two components in the J-band EPR spectra (cf. Figure 2.2), which differ with respect to the g_{xx} parameters. The spin label at position S118 possesses the largest g_{xx} (I) value and the largest relative contribution of that form, whereas in the mutant Q12C this component has a small contribution to the spectra. The mutants K27C and N42C are intermediate. For the K27C and the N42C mutants, the set of simulation parameters given in the table, i.e. the values of g_{xx} (I) and g_{xx} (II) and the respective spectral contributions, is not unique because of the strong interdependence of these parameters in the simulations.

We propose that the two spectral components are due to the spin label being exposed to slightly different micro-environments in the protein. Given that only the g_{xx}, and not the A_{zz} lines show two components, the two spectral components reveal that the spin-label environment corresponding to these components differs most with respect to the proticity and not the polarity of the protein. The magnitude of the splitting (Δg_{xx}) can be compared with models for the influence of hydrogen bonding and polarity on the spin label parameters[6,11,12]. These studies suggest, that the value of Δg_{xx} observed corresponds to one hydrogen bond (4×10^{-4} [6,11]) or a positive charge in the vicinity of the N-O-group of the spin label[11]. This would indicate that, in S118C, for one component, g_{xx} (I), the nitroxide group of the spin label is shielded from hydrogen bond donors, whereas for the other component, g_{xx} (II), it is exposed to a molecule or a group that can donate a hydrogen bond, such as a water molecule or an amino acid residue. For the other mutants, the weight of the component g_{xx} (I) decreases, as evidenced by the smaller percentage of the component with g_{xx} (I).

The nitroxide group can be exposed to different protein environments, if the linker connecting the spin label to the protein backbone has different conformations (rotamers), as has been proposed before. The X-ray structure of a spin-labeled protein[13] revealed different rotamers of the spin-label linker. The study [12] suggested that the two spectral components of these spin labels observed in EPR mobility studies were due to these groups of rotamers. We therefore propose that the two spectral components observed by J-band EPR correspond to different rotamers of the spin-label linker, which cause the spin label nitroxide group to have different hydrogen-bonding environments.

The present study reveals that small polarity/proticity differences can be resolved by high-field EPR. By increasing the field to 9 T in the novel 275 GHz spectrometer, two spectral components were observed that were previously not resolved in spin-labeled proteins. By comparing mobility studies[10] with the present investigation, subtle differences in the location of the

spin label can be resolved that will enable us to calibrate the result of molecular dynamics simulations and polarity calculations to be performed in the future.

Reference List

1. Steinhoff,H.J., Savitsky,A., Wegener,C., Pfeiffer,M. & Plato,M. High-field EPR studies of the structure and conformational changes of site-directed spin labeled bacteriorhodopsin. *Biochimica Et Biophysica Acta-Bioenergetics* **1457**, 253-262 (2000).

2. Lou,Y. & Ge,M.T. A multifrequency ESR study of the complex dynamics of membranes. *Journal of Physical Chemistry B* **105**, 11053-11056 (2001).

3. Altenbach,C., Marti,T., Khorana,H.G. & Hubbell,W.L. Transmembrane protein structure: spin labeling of bacteriorhodopsin mutants. *Science* **248**, 1088-1092 (1990).

4. Blok,H., Disselhorst,J.A.J.M. & Orlinskii,S.B. A continuous-wave and pulsed electron spin resonance spectrometer operating at 275 GHz. *Journal of Magnetic Resonance* **166**, 92-99 (2004).

5. van Amsterdam,I.M.C., Ubbink,M., Jeuken,L.J.C., Verbeet,M.P., Einsle,O. & Messerschmidt,A. Effects of dimerization on protein electron transfer. *Chemistry-A European Journal* **7**, 2398-2406 (2001).

6. Owenius,R., Engstrom,M., Lindgren,M. & Huber,M. Influence of solvent polarity and hydrogen bonding on the EPR parameters of a nitroxide spin label studied by 9-GHz and 95-GHz EPR spectroscopy and DFT calculations. *Journal of Physical Chemistry A* **105**, 10967-10977 (2001).

7. Finiguerra,M.G., Blok,H. & Ubbink,M. High-field (275 GHz) spin-label EPR for high-resolution polarity determination in proteins. *Journal of Magnetic Resonance* **180**, 197-202 (2006).

8. Nar,H., Messerschmidt,A., Huber,R., Vandekamp,M. & Canters,G.W. Crystal structure analysis of oxidized *Pseudomonas Aeruginosa* azurin at pH 5.5 and pH 9.0 - A pH-induced conformational transition involves a peptide bond flip. *Journal of Molecular Biology* **221**, 765-772 (1991).

9. van Amsterdam,I.M.C., Ubbink,M. & Canters,G.W. Anti-cooperativity in the two electron oxidation of the S118C disulfide dimer of azurin. *Inorganica Chimica Acta* **331**, 296-302 (2002).

10. Finiguerra,M.G., van Amsterdam,I.M.C., Alagaratnam,S. & Ubbink,M. Anisotropic spin label mobilities in azurin from 95 GHz electron paramagnetic resonance spectroscopy. *Chemical Physics Letters* **382**, 528-533 (2003).

11. Plato,M., Steinhoff,H.J., Wegener,C., Torring,J.T., Savitsky,A. & Möbius,K. Molecular orbital study of polarity and hydrogen bonding effects on the g and hyperfine tensors of site directed NO spin labelled bacteriorhodopsin. *Molecular Physics* **100**, 3711-3721 (2002).

12. Engstrom,M., Vaara,J., Schimmelpfennig,B. & Agren,H. Density functional theory calculations of electron paramagnetic resonance parameters of a nitroxide spin label in tissue factor and factor VIIa protein complex. *Journal of Physical Chemistry B* **106**, 12354-12360 (2002).

13. Hubbell,W.L., Gross,A., Langen,R. & Lietzow,M.A. Recent advances in site-directed spin labeling of proteins. *Current Opinion in Structural Biology* **8**, 649-656 (1998).